Current Biology 22, 695–700, April 24, 2012 ©2012 Elsevier Ltd All rights reserved DOI 10.1016/j.cub.2012.02.052

Report

Uridylation of miRNAs by HEN1 SUPPRESSOR1 in *Arabidopsis*

Guodong Ren,[1] Xuemei Chen,[2] and Bin Yu[1,*]
[1]Center for Plant Science Innovation and School of Biological Sciences, University of Nebraska, Lincoln, NE 68588–0660, USA
[2]Department of Botany and Plant Sciences, Institute of Integrative Genome Biology, University of California, Riverside, Riverside, CA 92521, USA

Summary

HEN1-mediated 2′-*O*-methylation has been shown to be a key mechanism to protect plant microRNAs (miRNAs) and small interfering RNAs (siRNAs) as well as animal piwi-interacting RNAs (piRNAs) from degradation and 3′ terminal uridylation [1–8]. However, enzymes uridylating unmethylated miRNAs, siRNAs, or piRNAs in *hen1* are unknown. In this study, a genetic screen identified a second-site mutation *hen1 suppressor1-2* (*heso1-2*) that partially suppresses the morphological phenotypes of the hypomorphic *hen1-2* allele and the null *hen1-1* allele in *Arabidopsis*. *HESO1* encodes a terminal nucleotidyl transferase that prefers to add untemplated uridine to the 3′ end of RNA, which is completely abolished by 2′-*O*-methylation. *heso1-2* affects the profile of u-tailed miRNAs and siRNAs and increases the abundance of truncated and/or normal sized ones in *hen1*, which often results in increased total amount of miRNAs and siRNAs in *hen1*. In contrast, overexpressing *HESO1* in *hen1-2* causes more severe morphological defects and less accumulation of miRNAs. These results demonstrate that HESO1 is an enzyme uridylating unmethylated miRNAs and siRNAs in *hen1*. These observations also suggest that uridylation may destabilize unmethylated miRNAs through an unknown mechanism and compete with 3′-to-5′ exoribonuclease activities in *hen1*. This study shall have implications on piRNA uridylation in *hen1* in animals.

Results

heso1-2 Partially Rescues the Morphological Phenotypes of *hen1-2* and *hen1-1*

In *Arabidopsis hen1-2*, an asparagine to aspartic acid substitution impaired HEN1 activity, reduced miRNA abundance, and caused pleiotropic developmental defects such as delayed growth and reduced fertility (short siliques) [9]. An ethyl methanesulfonate (EMS) mutagenized population of *hen1-2* was screened for second-site mutations that rescued the fertility defects of *hen1-2* [10]. This genetic screen was expected to identify components destroying unmethylated miRNAs because lack of them might increase the abundance of miRNAs and therefore suppress the fertility defects of *hen1-2*. NRPD1 and NRPD2/NRPE2, two essential genes for siRNA biogenesis, were identified from this screen [10–13].

We further screened the EMS mutagenized *hen1-2* population and isolated a suppressor with partially rescued vegetative phenotypes and longer siliques (Figures 1A and 1B). The average silique length of this suppressor was ~1.6-fold of that of *hen1-2* (Figures 1B and 1C). Backcross analysis revealed that a single recessive mutation caused the phenotypic changes in this suppressor. Following the nomenclature of the companion paper [14], the mutation was named *hen1 suppressor1-2* (*heso1-2*).

We next evaluated whether *heso1-2* suppressed *hen1-2* through restoring HEN1 activity. In this scenario, *heso1-2* should not suppress the null *hen1-1* allele. However, *hen1-1 heso1-2* grew better, produced longer siliques (~2-fold increase), and flowered earlier than *hen1-1* (Figures 1A–1C). To confirm that miRNA methylation status was not altered in *hen1-1 heso1-2*, we performed a periodate/β-elimination assay. Periodate/β-elimination treatment of unmethylated but not methylated miRNAs would result in faster migration during electrophoresis under denaturing condition, which could be detected by northern blot [15]. After chemical treatment, miR167 showed similar mobility alterations in *hen1-1 heso1-2* as in *hen1-1* (Figure S1). These results demonstrated that *heso1-2*-mediated phenotypic rescue of *hen1* did not require HEN1 methylase activity.

heso1-2 Partially Restores miRNA and *trans*-acting siRNA Function in *hen1-1*

The rescue of developmental defects of *hen1* by *heso1-2* could be best explained by the recovery of small RNA-mediated gene regulation, because dysregulation of small RNA targets was thought to be the major reason for the morphological phenotypes of *hen1* [16, 17]. We therefore compared the transcript levels of four miRNA targets, *CUC*, *PHV*, *HAP2b*, and *MYB65* and a *trans*-acting siRNA (ta-siRNA) target, *ARF3*, in *hen1-1 heso1-2* with those in *hen1-1* by quantitative RT-PCR (qRT-PCR) [17, 18]. As previously reported, their steady-state transcript levels were increased in *hen1-1* compared with those in L*er* plants (wild-type [WT] plants) [17, 18]. Relative to *hen1-1*, the transcript levels of these targets but not the control *UBQUITIN 5* were significantly reduced in *hen1-1 heso1-2* (Figure 1D). These results indicated that *heso1-2* might partially restore miRNA and ta-siRNA function in *hen1-1*.

heso1-2 Alters miRNA and siRNA Profiles in *hen1-2* and *hen1-1*

We next examined several miRNAs in *hen1-2*, *hen1-1*, *hen-1-1 heso1-2*, and *hen1-2 heso1-2* by northern blot. Tailed miRNAs were still present in *hen1-1 heso1-2* and *hen1-2 heso1-2* (Figure 2). To determine whether the tail consisted of untemplated Us in *hen1-1 heso1-2*, we performed a primer-extension analysis of miRNA-specific RT-PCR products amplified from miRNAs ligated to adaptors from *hen1-1 heso1-2* [2]. A ladder of primer-extension products was observed in both *hen1-1 heso1-2* and *hen1-1*, indicating the presence of U-tailed miRNA in *hen1-1 heso1-2* (Figure S2B). This result was consistent with the deep sequencing result in the companion paper [14].

Quantification analyses showed that *heso1-2* increased the total amounts of miR166/165, miR169, miR171/170, miR172, and miR173 in *hen1-1* and *hen1-2*, respectively (Figure 2), but not of miR167, whose overall levels had no obvious change

*Correspondence: byu3@unl.edu

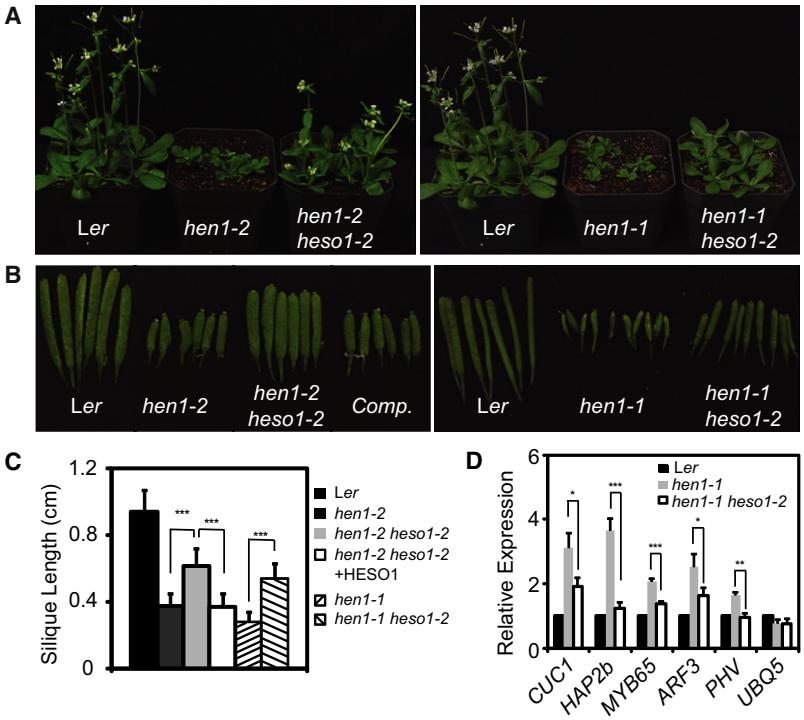

Figure 1. *heso1-2* Mutation Partially Suppresses the Phenotypes of *hen1-1* and *hen1-2*

(A) Morphological phenotypes of the indicated genotypes.

(B) Siliques from plants of the indicated genotypes. L*er* is WT plants. *hen1-1 heso1-2* and *hen1-2 heso1-2* are *hen1-1* and *hen1-2* harboring the *heso1-2* mutation, respectively. *Comp* is *hen1-2 heso1-2* harboring the *HESO1* genomic DNA.

(C) Average silique length in various genotypes. Thirty siliques from six plants for each genotype were included in the analysis. ***p < 0.001.

(D) The transcript levels of miRNA and ta-siRNA targets in various genotypes. Target mRNA accumulation in various genotypes was quantified by qRT-PCR and compared with those of WT. Quantifications are normalized with *ACTIN2* transcript. *UBQ5*: *UBQUITIN5*, which served as an internal control. The WT value is 1. *p < 0.05; **p <0.01; ***p < 0.001.

(Figure 2). *heso1-2* appeared to have a greater effect in *hen1-1* than *hen1-2*, presumably due to the fact that *hen1-1* is a null allele, whereas *hen1-2* is a weak allele (Figure 2). For the examined miRNAs, truncated forms were increased in abundance in *hen1-1 heso1-2* (2.2- to 4.3-fold of those in *hen1-1*) and *hen1-2 heso1-2* (1.8- to 6.8-fold of those in *hen1-2*), compared with *hen1-1* and *hen1-2*, respectively (Figure 2; Figure S2A). Sequencing analysis of miR167 demonstrated that truncations occurred at 3′ end (Table S1), in agreement with deep-sequencing analysis results in the companion paper [14]. The normal-sized miR169, miR171, miR172, and miR173 were increased in accumulation as well by *heso1-2* in *hen1-1* and *hen1-2*, respectively (Figure 2; Figure S2). *heso1-2* also appeared to reduce the abundance of tailed miR167 and miR166/165 (>21 nt for miR167, >22 nt for miR166/165; Figure 2; Figure S2A). Although the levels of short-tailed miR171 (22–23 nt), miR172 (23–24 nt), and miR173 (23–24 nt) were increased by *heso1-2* in *hen1-1* and *hen1-2*, the abundance of longer ones (>24 nt for miR171, >25 nt for miR172 and miR173) was reduced (Figure 2; Figure S2A). These results suggested that *heso1-2* increases the levels of normal-sized, 3′ truncated, and/or short-tailed miRNAs in *hen1*, which often led to an increase of the total amount of miRNAs.

We next examined the accumulation of a heterochromatic siRNA siR02 and a *trans*-acting siRNA TAS3-5′D8(+). *heso1-2* increased the total amount of TAS3-5′D8(+), which lacks detectable U-tailed forms in *hen1* and double mutants, but not siR02 (Figure 2). However, *heso1-2* did increase the abundance of normal-sized and truncated siR02 and reduced accumulation of tailed isoforms in *hen1-1* and *hen1-2* (Figure 2).

We also evaluated the effect of *heso1-2* mutation on miRNA accumulation in WT. However, northern blot showed that the levels of miR167, miR171, and miR173 in *heso1-2* are comparable with those in WT (Figure S2C).

HESO1 Encodes a Cytoplasm and Nucleus-Localized Terminal Nucleotidyl Transferase

We next used a map-based cloning approach to determine the molecular nature of *heso1-2* mutation. The mapping population was constructed by crossing *hen1-2 heso1-2* with *hen1-8*, which carries the same mutation as *hen1-2* but is in the Columbia-0 genetic background [10]. In the F2 segregating population, the plants with longer siliques were selected for marker analysis. The *heso1-2* mutation was mapped to a ~70 kb region of chromosome 2 on the bacterial artificial chromosome (BAC) T5I7 (Figure S3A). Sequencing analysis of this region revealed a G-to-A change at the end of fifth intron of the gene At2g39740 (Figures S3B and S3C). Introduction of a WT genomic DNA covering At2g39740 promoter and coding regions into *hen1-2 heso1-2* was able to restore miRNA and fertility phenotypes of *hen1-2* (Figures 1B and 1C; Figure S3E). These results demonstrated that the G-to-A mutation in At2g39740 was responsible for the partial rescue of *hen1-2*. We named At2g39740 HEN1 SUPPRESSOR1 (HESO1). HESO1 encodes a putative nucleotidyl transferase that belongs to the DNA polymerase β-like superfamily [19]. It contains a poly A polymerase domain, (PAP/25A), a PAP-associated domain, and a glutamine rich region (Figure 3A). However HESO1 is distinct from canonical, eukaryotic PAPs because it lacks the RNA-binding motif (RRM) of classical PAP. HESO1 is thought to be a member of GLD-2-related family that adds nucleotides to the 3′ end of RNAs independent of templates [20].

RT-PCR and subsequent sequencing analyses detected four abnormal but no WT *HESO1* transcripts in *hen1-2 heso1-2* (Figure S3D), indicating that the G-to-A mutation caused splicing defects. Either intron 5 was fully retained in the messenger RNA (mRNA) (transcript 1) or exon 6 was partially (transcript 2 and 3) or completely spliced out (transcript 4; Figure S3D). Transcripts 1, 2, and 4 contained in-frame stop codons, which should lead to the production of truncated proteins lacking the C-terminal region starting from amino acid 194 (Figure 3A; Figure S3D). Transcript 3 was predicted to produce a mutant protein, in which 16 amino acids (194–209) including the last 4 amino acids of PAP/5A core region were deleted (Figure 3A; Figure S3D). This deletion completely abolished nucleotidyl transferase activity of HESO1 (Figure 3B, described below). Thus, *heso1-2* is most likely a null allele.

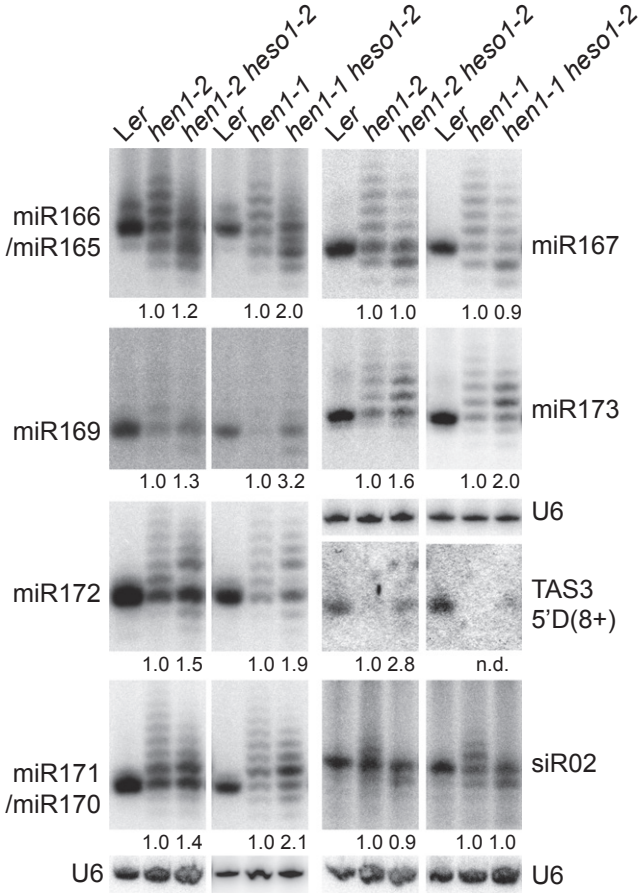

Figure 2. *heso1-2* Affects miRNA and siRNA Profiles in *hen1-1* and *hen1-2*

miRNAs and siRNAs in various genotypes were monitored by northern blot. U6 was used as a loading control. L*er* served as a size control. miR166/165 and miR171/170, the paired miRNAs were recognized by the same probe because of sequence similarities.

The number below *hen1-1 heso1-2* and *hen1-2 heso1-2* indicated the fold changes of total amounts of miRNAs or siRNAs caused by *heso1-2* in *hen1-1* and *hen1-2*, respectively. n.d. represents not detected in *hen1-1*. To obtain the total amount of a miRNA and siRNA in each genotype, we quantified all individual bands in each sample and added them together. The total amount of a miRNA and siRNA in *hen1-1 heso1-2* and *hen1-2 heso1-2* was then normalized to U6 RNA and compared with that in *hen1-1* and *hen1-2*, respectively.

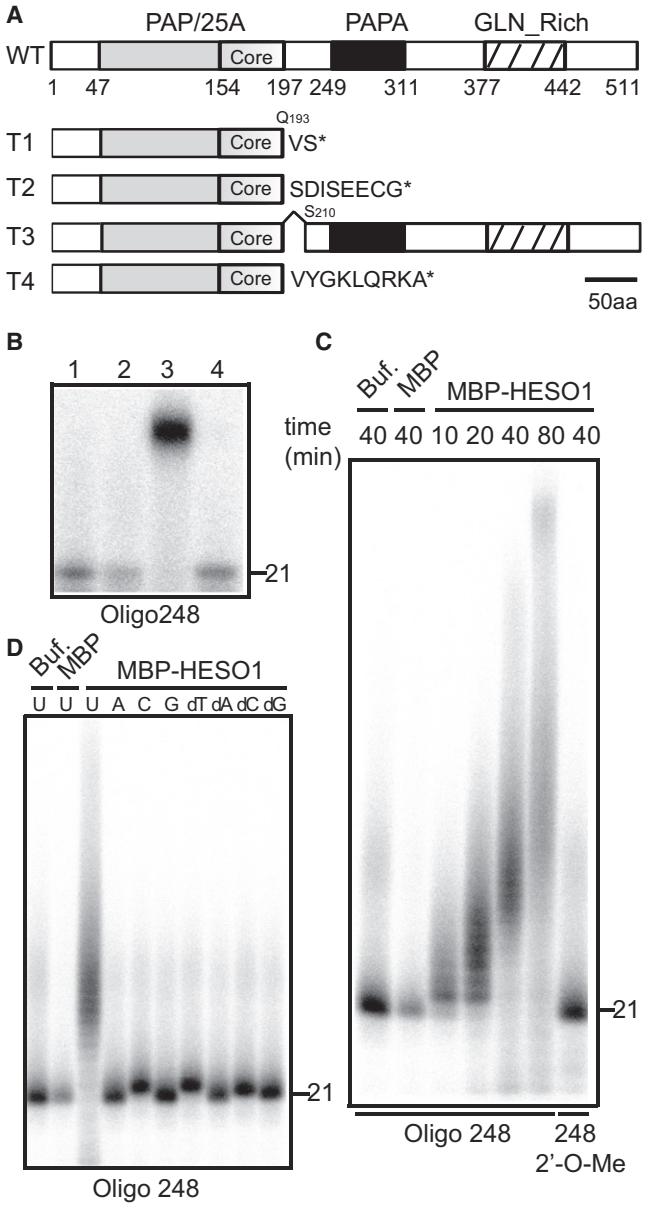

Figure 3. HESO1 Encodes a 3′ Terminal Uridylyl Transferase

(A) Schematic of HESO1 protein and its mutant forms generated by *heso1-2*. * represents protein stop codon. The amino acids introduced by *heso1-2* following the truncated HESO1 are indicated. PAP/25A, poly A polymerase domain; PAPA, PAP associated domain; Core, core regions of PAP/25A; GLN_RICH, glutamine rich region.

(B) Terminal uridylyl transferase activity of HESO1. Oligo 248 was 5′-end labeled with P^{32}, incubated with buffer alone (1), purified MBP (2), MBP-HESO1 (3) or MBP-HESO1Δ16 (4) under the presence of UTP for 120 min, and resolved on a denaturing polyacrylamide gel.

(C) Time-course reaction of HESO1 activity and the effect of 2′-*O*-methylation on HESO1 activity. 5′ end–labeled oligo 248 or 2′-*O*-methyl oligo 248 was incubated with MBP-HESO1. The reaction was stopped at the indicated time.

(D) Preference of HESO1 to ribonucleotides and deoxyribonucleotides. 5′ end labeled oligo 248 was incubated with MBP-HESO1 under the presence of UTP, ATP, CTP, GTP, dATP, dTTP, dCTP, or dGTP for 40 min.

The alteration of U-tailing profile of small RNAs in *hen1 heso1-2* together with the protein annotation suggested that HESO1 might be an enzyme responsible for the untemplated uridine addition to the 3′ end of miRNAs and siRNAs in *hen1*. Therefore, we tested whether HESO1 possessed terminal nucleotidyl transferase activity using a recombinant maltose-binding protein (MBP)-HESO1 protein. The recombinant MBP-HESO1 was expressed in *E. coli* and purified with maltose resin (Figure S3F). As controls, a MBP protein and a MBP-HESO1 protein lacking amino acid from 194 to 209 (MBP-HESO1Δ16 encoded by the transcript 3 in *hen1-2 heso1-2*, Figure S3F) were also expressed. We incubated the proteins with an in vitro synthesized 21 nt oligo RNA (oligo 248) [21], which was 5′ P^{32}-labeled, under the presence of uridine triphosphate (UTP). After the reaction was stopped, the RNA was resolved on a polyacrylamide gel. MBP-HESO1 but not MBP and MBP-HESO1Δ16 lengthened the substrate RNA (Figure 3B), indicating that HESO1 added untemplated uridines to the 3′ end of oligo 248. A time-course experiment revealed that the RNA substrate was elongated during the

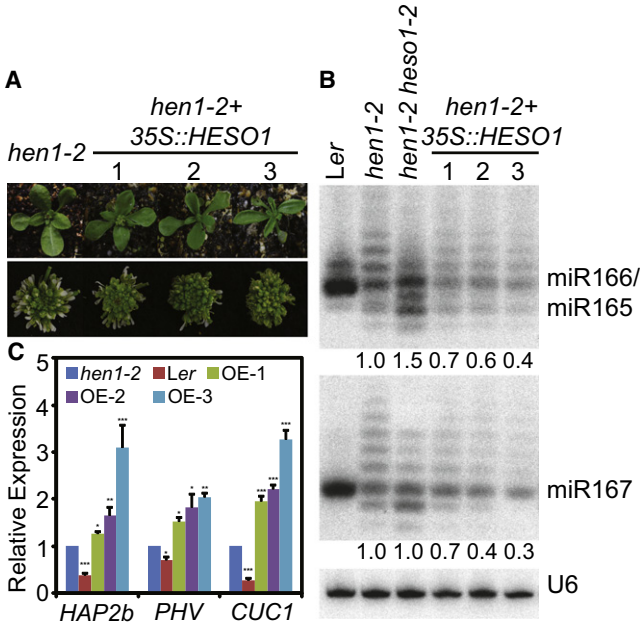

Figure 4. Overexpression of *HESO1* in *hen1-2* Causes More Severe Phenotypes

(A) Morphological phenotypes of various genotypes. L*er* is WT plants. *hen1-2 + 35S::HESO1* is *hen1-2* overexpressing *HESO1*.

(B) miR167 and miR166/165 in various genotypes were monitored by northern blot. U6 was used as a loading control. L*er* served as a miRNA size control; *hen1-2 + 35S::HESO1*, *hen1-2* overexpressing *HESO1*. The number below overexpression lines indicated the fold changes of total amounts of miRNAs or siRNAs caused by overexpression of *HESO1* in *hen1-2*, respectively. To obtain the total amount of a miRNA and siRNA in each genotype, we quantified all individual bands in each sample and added them together. The total amount of a miRNA and siRNA in *HESO1* overexpression lines *2* was then normalized to U6 RNA and compared with that in *hen1-2*.

(C) The transcript levels of three miRNA targets in L*er*, *hen1-2*, and three *HESO1* overexpression lines. Target mRNA accumulation in various genotypes was quantified by qRT-PCR and compared with those of WT. Quantifications are normalized with *ACTIN2* transcript. The *hen1-2* value is 1. *$p < 0.05$; **$p < 0.01$; ***$p < 0.001$.

reaction (Figure 3C), demonstrating that HESO1 had template-independent polymerase activity. A 2′-*O*-methyl group at the 3′ end of oligo 248 completely abolished HESO1 activity (Figure 3C), which is consistent with the notion that methylation prevents 3′ uridylation of plant miRNAs and siRNAs and animal piRNAs [1, 2, 8]. MBP-HESO1 was able to add one cytidine (C), deoxythymidine (dT), or deoxycytidine (dC) to the 3′ end of oligo 248 (Figure 3D). The results demonstrated that HESO1 has preference to add Us to the 3′ end of RNA under our assay conditions.

In order to examine the localization of HESO1 in cells, we transiently expressed *HESO1* under the control of a Cauliflower mosaic virus (CaMV) 35S promoter in *Nicotiana benthamiana* [22]. The transgene was able to produce functional protein because it caused more severe defects of *hen1-2* when expressed (described below). The yellow florescence signal could be observed in both cytoplasm and nucleus in the leaf epidermal cells of *N. benthamiana* harboring *35S::HESO1-YFP* (Figure S3G), suggesting that HESO1 might be localized in both cytoplasm and nucleus, consistent with the observation that both miRNAs and siRNAs were affected by *heso1-2* in *hen1-1* and *hen1-2*.

Overexpression of *HESO1* in *hen1-2* Causes More Severe Morphological Defects and Less miRNA Accumulation

The fact that lack of HESO1 in *hen1* increased the accumulation of miRNAs suggested that HESO1-mediated uridylation might destabilize unmethylated miRNAs. If so, we would expect that overexpression of *HESO1* in *hen1* could further reduce the abundance of miRNAs and cause more severe developmental defects. We overexpressed *HESO1* under the control of 35S promoter in *hen1-2*. In T1 transgenic plants, three transgenic *hen1-2 heso1-2* with 4- to 12-fold increased transcript levels of *HESO1* relative to *hen1-2* were selected by qRT-PCR analysis (Figure S4). All of these three transgenic lines showed more severe leaf and flower morphological defects than *hen1-2* (Figure 4A). Northern blot analysis revealed that the amount of miR166/165 and miR167 was reduced in three transgenic *hen1-2* lines overexpressing *HESO1* compared with *hen1-2* (Figure 4B). This result supported that HESO1 might trigger degradation of unmethylated miRNAs. Furthermore, we detected increased miRNA target transcript levels in overexpression lines relative to *hen1-2* (Figure 4C), indicating that the reduction of miRNA abundance may be the cause for severe morphological defects of overexpression lines.

Discussion

The in vitro uridylyl transferase activity of HESO1 and the effect of *heso1-2* on the profile of uridylated small RNAs in *hen1* demonstrate that HESO1 is an enzyme targeting unmethylated miRNAs and siRNAs in *hen1*. The facts that *heso1-2* increases the levels of miRNAs and overexpression of *HESO1* reduces the abundance of miRNAs in *hen1* demonstrate the hypothesis that uridylation triggers degradation of plant miRNAs and siRNAs or animal piRNAs in *hen1* [1–4, 8, 21, 23]. It has been observed that uridylation triggers the degradation of miRNAs from 3′ end by exosome component RRP6 in vitro in *Chlamydomonas* [21]. However, the increased accumulation of 3′ truncated miRNAs and siRNAs in *hen1 heso1-2* indicates that mechanisms other than 3′-to-5′ degradation might be employed by *Arabidopsis* to degrade uridylated miRNA and siRNAs. It is possible that uridylation may trigger highly progressive 3′-to-5′ degradation so that the 3′ truncated products was less accumulated in *hen1*. The presence of 3′ truncated miRNAs and siRNAs in *hen1* also indicates that 3′-to-5′ degradation activities such as SDN1, exosome or homologs of Nibbler might act on miRNAs and siRNAs in *hen1* as well [21, 24–26]. It is tempting to speculate that HESO1 may compete with 3′-to-5′ exoribonuclease activities or their products as substrates in *Arabidopsis*.

Additional terminal uridylyl transferases must act in miRNA and siRNA uridylation processes in *hen1* because uridylated miRNAs and siRNAs are still present in *hen1 heso1-2* and *heso1-2* is most likely a null allele. *Arabidopsis* encodes nine additional HESO1 homologs (Figure S3H). One or more of them may add U tails to the unmethylated small RNAs in *hen1 heso1-2*. The increased accumulation of some miRNAs with short tails is observed in *hen1 heso1-2*. A possible explanation is that other nucleotidyl transferases may add a short tail to miRNA, which then can be used by HESO1 as substrates to elongate. However, other possibilities are also present. This observation also suggests that the short-tailed miRNAs may have a very slow degradation rate, or a certain U tail length threshold may be required to trigger degradation in *Arabidopsis*. The reduced abundance of U-tailed

miR166/165 and miR167 may reflect substrate preference of HESO1 homologs. Consistent with this, terminal nucleotidyl transferases GLD-2 and ZCCHC11 have been shown to specifically modify miR122 and miR26 in animals, respectively [27, 28]. Several putative terminal nucleotidyl transferases are also proposed to modify miRNAs in a miRNA-specific manner in human [29].

heso1-2 has no obvious effect on several examined miRNAs in WT, indicating that 2′-*O*-methylation prevents HESO1 activity. However, we cannot rule out the possibility that HESO1 has subtle effects on small RNA levels. In fact, tailed miRNAs and siRNAs are also present in WT plants [2]. In addition to miRNAs and siRNAs, HESO1 may have other substrates in vivo such as 5′ fragments of RNA-induced silencing complex cleavage products, U6 small nuclear RNA and ribosomal 5S RNAs. Uridylation of these RNAs has been established [30–32]. In animals, uridylation of pre-let7 is also observed [33–35]. Clearly, these possibilities need to be examined in the future.

Supplemental Information

Supplemental Information includes four figures, two tables, and Supplemental Experimental Procedures and can be found with this article online at doi:10.1016/j.cub.2012.02.052.

Acknowledgments

We thank Xiang Liu, Shuxin Zhang, Meng Xie, and Heriberto Cerutti from the University of Nebraska Lincoln for critical reading of the manuscript and Heriberto Cerutti for providing RNA oligo 248 and 2′-*O*-methyalted oligo 248. This work was supported by National Science Foundation (NSF) MCB-1121193 (to B.Y.), a faculty seed grant and an Enhancing Interdisciplinary Teams Grant from the University of Nebraska Lincoln (to B.Y.), and NSF MCB-1021465 (to X.C.).

Received: January 24, 2012
Revised: February 16, 2012
Accepted: February 21, 2012
Published online: March 29, 2012

References

1. Kamminga, L.M., Luteijn, M.J., den Broeder, M.J., Redl, S., Kaaij, L.J., Roovers, E.F., Ladurner, P., Berezikov, E., and Ketting, R.F. (2010). Hen1 is required for oocyte development and piRNA stability in zebrafish. EMBO J. *29*, 3688–3700.
2. Li, J., Yang, Z., Yu, B., Liu, J., and Chen, X. (2005). Methylation protects miRNAs and siRNAs from a 3′-end uridylation activity in Arabidopsis. Curr. Biol. *15*, 1501–1507.
3. Horwich, M.D., Li, C., Matranga, C., Vagin, V., Farley, G., Wang, P., and Zamore, P.D. (2007). The Drosophila RNA methyltransferase, DmHen1, modifies germline piRNAs and single-stranded siRNAs in RISC. Curr. Biol. *17*, 1265–1272.
4. Saito, K., Sakaguchi, Y., Suzuki, T., Suzuki, T., Siomi, H., and Siomi, M.C. (2007). Pimet, the Drosophila homolog of HEN1, mediates 2′-*O*-methylation of Piwi- interacting RNAs at their 3′ ends. Genes Dev. *21*, 1603–1608.
5. Kirino, Y., and Mourelatos, Z. (2007). The mouse homolog of HEN1 is a potential methylase for Piwi-interacting RNAs. RNA *13*, 1397–1401.
6. Kirino, Y., and Mourelatos, Z. (2007). Mouse Piwi-interacting RNAs are 2′-*O*-methylated at their 3′ termini. Nat. Struct. Mol. Biol. *14*, 347–348.
7. Ohara, T., Sakaguchi, Y., Suzuki, T., Ueda, H., Miyauchi, K., and Suzuki, T. (2007). The 3′ termini of mouse Piwi-interacting RNAs are 2′-*O*-methylated. Nat. Struct. Mol. Biol. *14*, 349–350.
8. Ameres, S.L., Horwich, M.D., Hung, J.H., Xu, J., Ghildiyal, M., Weng, Z., and Zamore, P.D. (2010). Target RNA-directed trimming and tailing of small silencing RNAs. Science *328*, 1534–1539.
9. Chen, X., Liu, J., Cheng, Y., and Jia, D. (2002). HEN1 functions pleiotropically in Arabidopsis development and acts in C function in the flower. Development *129*, 1085–1094.
10. Yu, B., Bi, L., Zhai, J., Agarwal, M., Li, S., Wu, Q., Ding, S.W., Meyers, B.C., Vaucheret, H., and Chen, X. (2010). siRNAs compete with miRNAs for methylation by HEN1 in Arabidopsis. Nucleic Acids Res. *38*, 5844–5850.
11. Herr, A.J., Jensen, M.B., Dalmay, T., and Baulcombe, D.C. (2005). RNA polymerase IV directs silencing of endogenous DNA. Science *308*, 118–120.
12. Onodera, Y., Haag, J.R., Ream, T., Costa Nunes, P., Pontes, O., and Pikaard, C.S. (2005). Plant nuclear RNA polymerase IV mediates siRNA and DNA methylation-dependent heterochromatin formation. Cell *120*, 613–622.
13. Pontier, D., Yahubyan, G., Vega, D., Bulski, A., Saez-Vasquez, J., Hakimi, M.A., Lerbs-Mache, S., Colot, V., and Lagrange, T. (2005). Reinforcement of silencing at transposons and highly repeated sequences requires the concerted action of two distinct RNA polymerases IV in Arabidopsis. Genes Dev. *19*, 2030–2040.
14. Zhao, Y., Yu, Y., Zhai, J., Ramachandran, V., Dinh, T.T., Meyers, B.C., Mo, B., and Chen, X. (2012). The A*rabidopsis* nucleotidyl transferase HESO1 uridylates unmethylated small RNAs to trigger their degradation. Curr. Biol. *22*, 689–694.
15. Yu, B., Yang, Z., Li, J., Minakhina, S., Yang, M., Padgett, R.W., Steward, R., and Chen, X. (2005). Methylation as a crucial step in plant microRNA biogenesis. Science *307*, 932–935.
16. Boutet, S., Vazquez, F., Liu, J., Béclin, C., Fagard, M., Gratias, A., Morel, J.B., Crété, P., Chen, X., and Vaucheret, H. (2003). Arabidopsis HEN1: a genetic link between endogenous miRNA controlling development and siRNA controlling transgene silencing and virus resistance. Curr. Biol. *13*, 843–848.
17. Vaucheret, H., Vazquez, F., Crété, P., and Bartel, D.P. (2004). The action of ARGONAUTE1 in the miRNA pathway and its regulation by the miRNA pathway are crucial for plant development. Genes Dev. *18*, 1187–1197.
18. Allen, E., Xie, Z., Gustafson, A.M., and Carrington, J.C. (2005). microRNA-directed phasing during trans-acting siRNA biogenesis in plants. Cell *121*, 207–221.
19. Aravind, L., and Koonin, E.V. (1999). DNA polymerase beta-like nucleotidyltransferase superfamily: identification of three new families, classification and evolutionary history. Nucleic Acids Res. *27*, 1609–1618.
20. Kwak, J.E., and Wickens, M. (2007). A family of poly(U) polymerases. RNA *13*, 860–867.
21. Ibrahim, F., Rymarquis, L.A., Kim, E.J., Becker, J., Balassa, E., Green, P.J., and Cerutti, H. (2010). Uridylation of mature miRNAs and siRNAs by the MUT68 nucleotidyltransferase promotes their degradation in Chlamydomonas. Proc. Natl. Acad. Sci. USA *107*, 3906–3911.
22. Kapila, J., de Rycke, R., van Montagu, M., and Angenon, G. (1997). An Agrobacterium-mediated transient gene expression system or intact leaves. Plant Sci. *122*, 101–108.
23. van Wolfswinkel, J.C., Claycomb, J.M., Batista, P.J., Mello, C.C., Berezikov, E., and Ketting, R.F. (2009). CDE-1 affects chromosome segregation through uridylation of CSR-1-bound siRNAs. Cell *139*, 135–148.
24. Ramachandran, V., and Chen, X. (2008). Degradation of microRNAs by a family of exoribonucleases in Arabidopsis. Science *321*, 1490–1492.
25. Han, B.W., Hung, J.H., Weng, Z., Zamore, P.D., and Ameres, S.L. (2011). The 3′-to-5′ exoribonuclease Nibbler shapes the 3′ ends of microRNAs bound to Drosophila Argonaute1. Curr. Biol. *21*, 1878–1887.
26. Liu, N., Abe, M., Sabin, L.R., Hendriks, G.J., Naqvi, A.S., Yu, Z., Cherry, S., and Bonini, N.M. (2011). The exoribonuclease Nibbler controls 3′ end processing of microRNAs in Drosophila. Curr. Biol. *21*, 1888–1893.
27. Katoh, T., Sakaguchi, Y., Miyauchi, K., Suzuki, T., Kashiwabara, S., Baba, T., and Suzuki, T. (2009). Selective stabilization of mammalian microRNAs by 3′ adenylation mediated by the cytoplasmic poly(A) polymerase GLD-2. Genes Dev. *23*, 433–438.
28. Jones, M.R., Quinton, L.J., Blahna, M.T., Neilson, J.R., Fu, S., Ivanov, A.R., Wolf, D.A., and Mizgerd, J.P. (2009). Zcchc11-dependent uridylation of microRNA directs cytokine expression. Nat. Cell Biol. *11*, 1157–1163.
29. Wyman, S.K., Knouf, E.C., Parkin, R.K., Fritz, B.R., Lin, D.W., Dennis, L.M., Krouse, M.A., Webster, P.J., and Tewari, M. (2011). Post-transcriptional generation of miRNA variants by multiple nucleotidyl transferases contributes to miRNA transcriptome complexity. Genome Res. *21*, 1450–1461.
30. Shen, B., and Goodman, H.M. (2004). Uridine addition after microRNA-directed cleavage. Science *306*, 997.

31. Chen, Y., Sinha, K., Perumal, K., and Reddy, R. (2000). Effect of 3′ terminal adenylic acid residue on the uridylation of human small RNAs in vitro and in frog oocytes. RNA *6*, 1277–1288.
32. Ibrahim, F., Rohr, J., Jeong, W.J., Hesson, J., and Cerutti, H. (2006). Untemplated oligoadenylation promotes degradation of RISC-cleaved transcripts. Science *314*, 1893.
33. Hagan, J.P., Piskounova, E., and Gregory, R.I. (2009). Lin28 recruits the TUTase Zcchc11 to inhibit let-7 maturation in mouse embryonic stem cells. Nat. Struct. Mol. Biol. *16*, 1021–1025.
34. Lehrbach, N.J., Armisen, J., Lightfoot, H.L., Murfitt, K.J., Bugaut, A., Balasubramanian, S., and Miska, E.A. (2009). LIN-28 and the poly(U) polymerase PUP-2 regulate let-7 microRNA processing in Caenorhabditis elegans. Nat. Struct. Mol. Biol. *16*, 1016–1020.
35. Heo, I., Joo, C., Kim, Y.K., Ha, M., Yoon, M.J., Cho, J., Yeom, K.H., Han, J., and Kim, V.N. (2009). TUT4 in concert with Lin28 suppresses microRNA biogenesis through pre-microRNA uridylation. Cell *138*, 696–708.